Electronic Supporting Information

Theoretical Insights into Nonprecious Oxygen-Evolution Active Sites in Ti-Ir-Based Perovskite Solid Solution Electrocatalysts

Lei Shi‡, Hui Chen‡, Xiao Liang, Yipu Liu, Xiaoxin Zou*

State Key Laboratory of Inorganic Synthesis and Preparative Chemistry, College of Chemistry, Jilin University, Changchun 130012, P. R. China

‡ Lei Shi and Hui Chen contributed equally to this work.

*Corresponding author. E-mail: xxzou@jlu.edu.cn

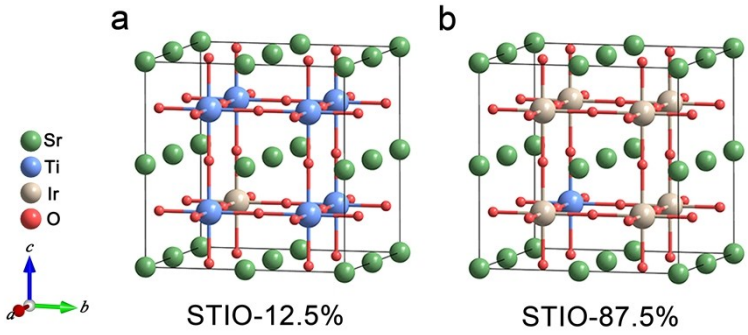

Fig. S1. The structural models of **a,** STIO-12.5%, **b,** STIO-87.5%. The models with remain iridium content are shown in Table S1, because of their various possible doping configurations.

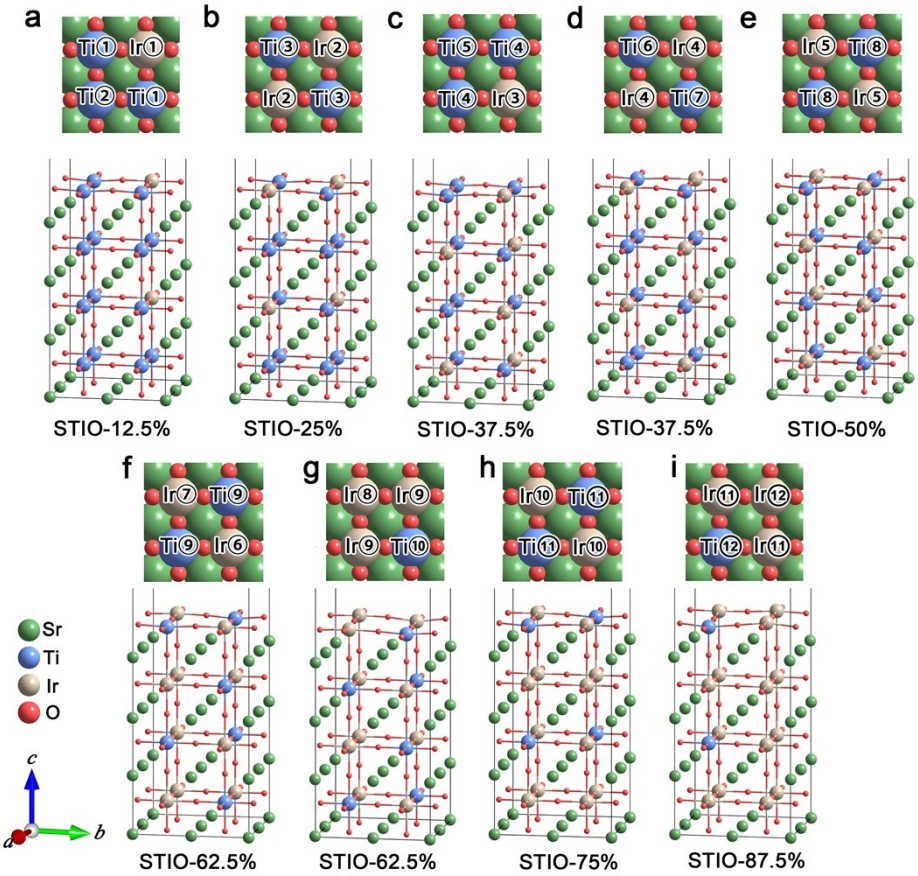

Fig. S2. Structural models and the corresponding top views for the (001) planes of **a,** STIO-12.5%, **b,** STIO-25%, **c, d,** STIO-37.5%, **e,** STIO-50% **f, g**, STIO-62.5%, **h,** STIO-75%, **i,** STIO-87.5%. The titanium and iridium sites with different atomic environments are marked on the top views, and the corresponding free energy for the intermediates are shown in Table S3 and Table S4, respectively.

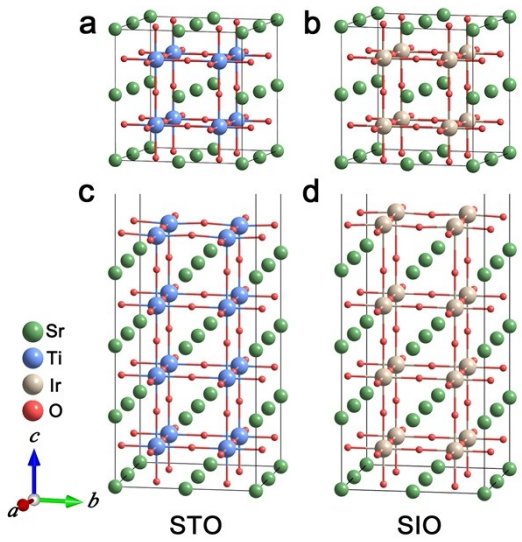

Fig. S3. a, b, $SrTiO_3$ and $SrIrO_3$ supercells with the cubic structure. **c,** The slab model for the (001) plane of the STO. **d,** The slab model for the (001) plane of the SIO. The free energy for the intermediates on Ti/Ir sites are shown in Table S3 and Table S4, respectively.

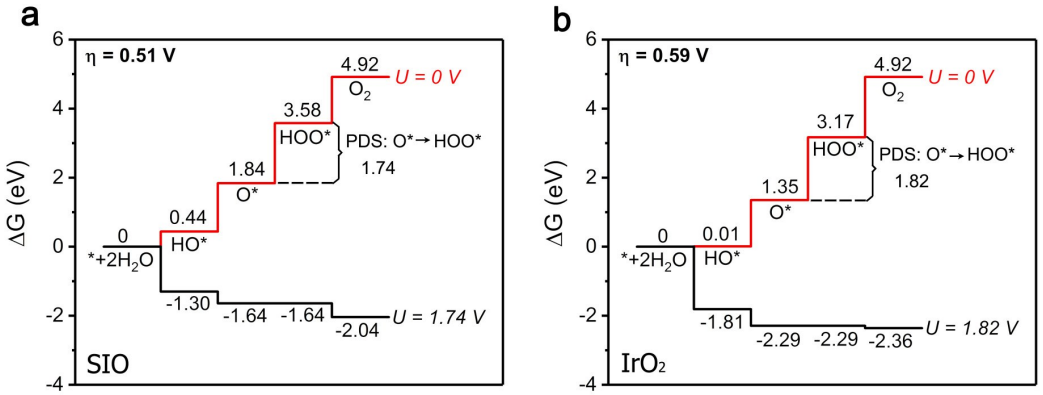

Fig. S4. The Gibbs free energy diagram for (a) SIO and (b) IrO_2, respectively. The data for IrO_2 are taken from our previous study. Ref. [1]. The overpotential of perovskite SIO (0.51 V) are lower than that of rutile IrO_2 (0.59 V) because of the weaker bonding energy of the intermediates on the SIO.

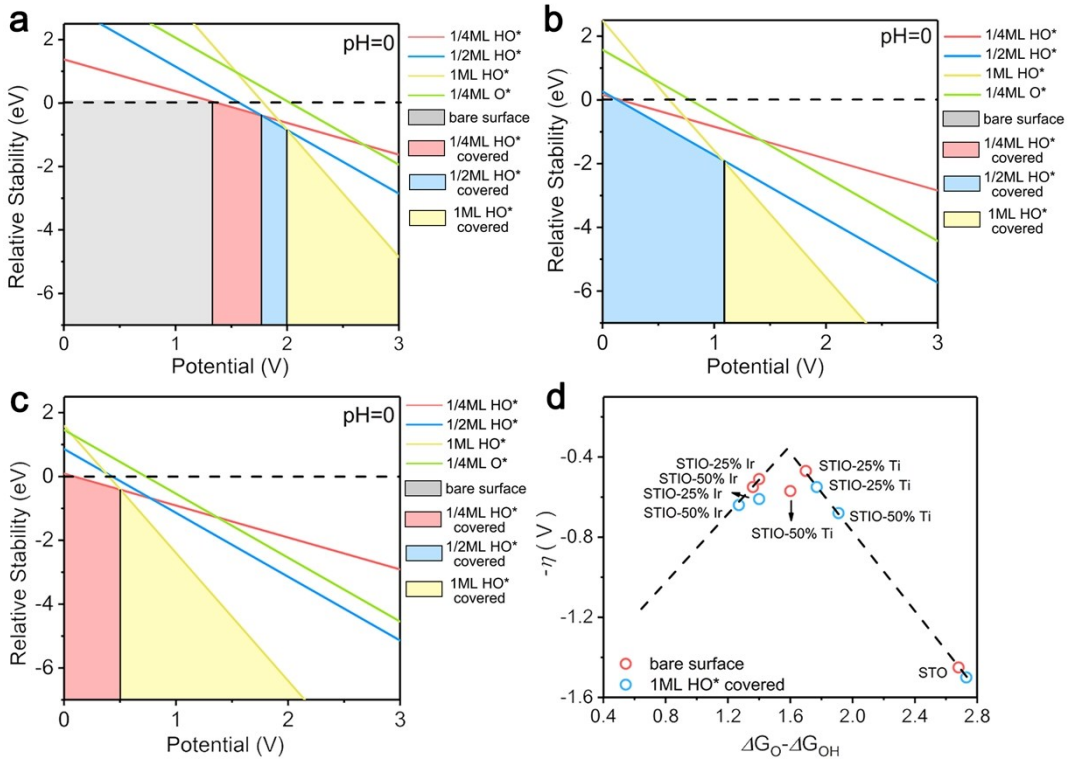

Fig. S5. The surface phase diagram for (a) STO, (b) STIO-25% and (c) STIO-50% respectively. (d) The Volcano-type plot of OER activities for the corresponding Ti and Ir sites on the bare surface and the 1ML HO* covered surface. The free energy for the intermediates are shown in Table S5.

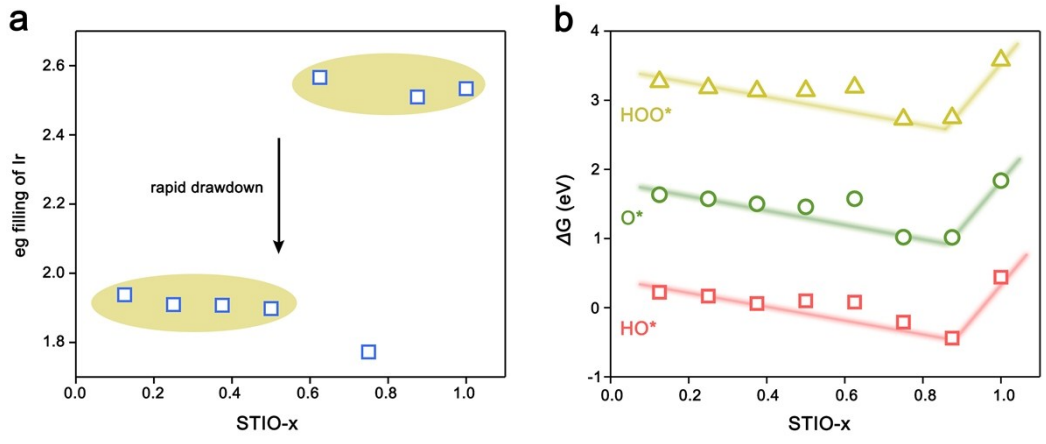

Fig. S6. (a) The e_g-filling and (b) adsorption free energy of HOO*, O* and HO* for the most active iridium sites plotted as a function of the iridium content of STIO.

The adsorption energy values of the three intermediates of the surface iridium sites for STIO with iridium from12.5% to 62.5% shows the similar energy as the pure SIO, and decrease at high iridium content, while the eg-filling for the iridium sites with iridium content from 50% to 87.5% is similar with the pure SIO and rapid draw down as iridium content decrease to lower than 50%.

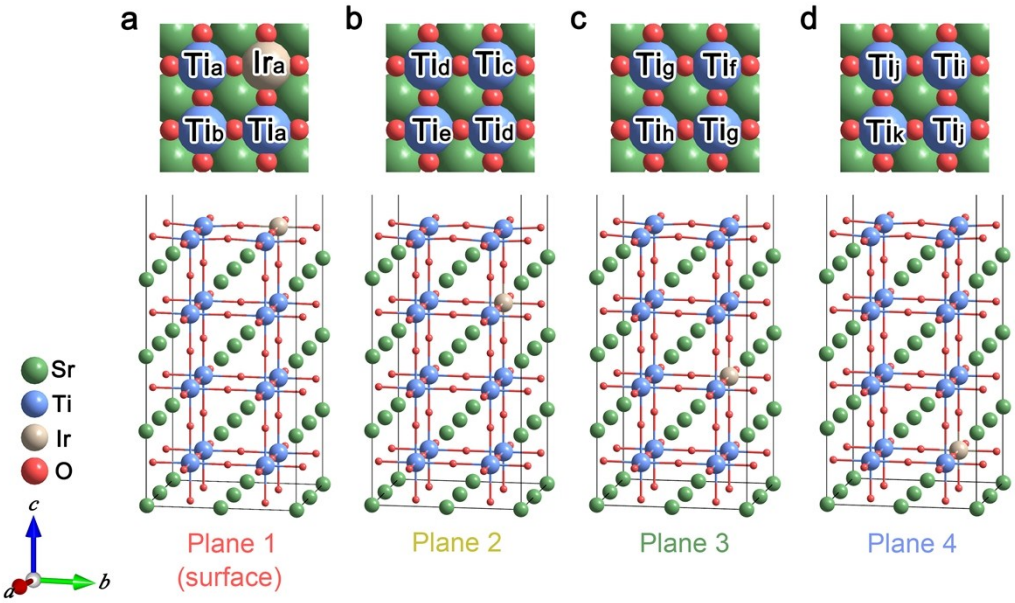

Fig. S7. Structural models and the corresponding top views of STO slab models with iridium doped in **a,** Plane 1 (surface), **b,** Plane 2, **c,** Plane 3, **d,** Plane 4. The titanium and iridium sites with different atomic environments are marked on the top views, and the corresponding free energy for the intermediates are shown in Table S6.

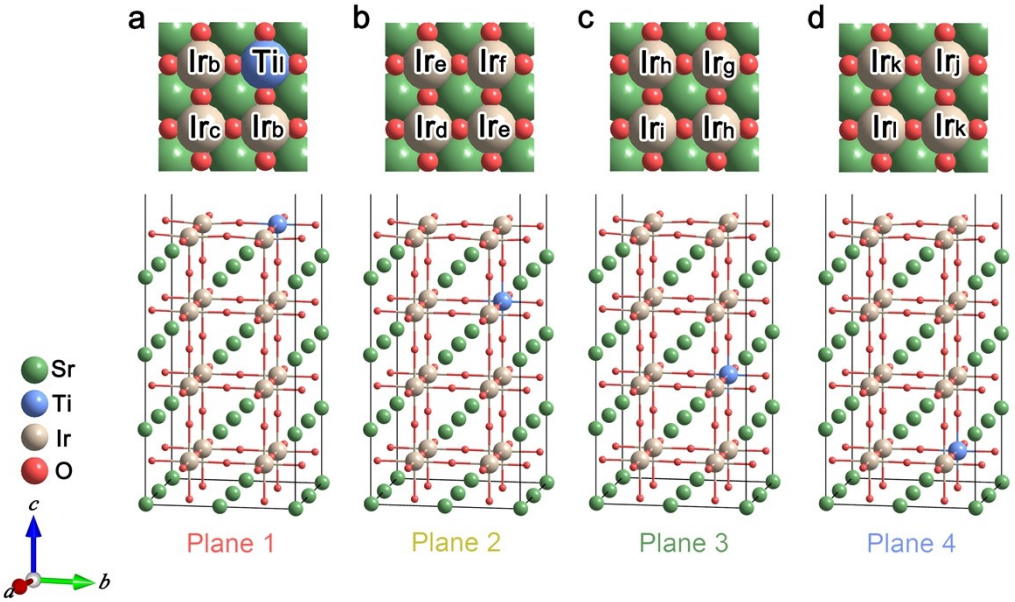

Fig. S8. Structural models and the corresponding top views of SIO slab models with titanium doped in **a,** Plane 1 (surface), **b,** Plane 2, **c,** Plane 3, **d,** Plane 4. The titanium and iridium sites with different atomic environments are marked on the top views, and the corresponding free energy for the intermediates are shown in Table S7.

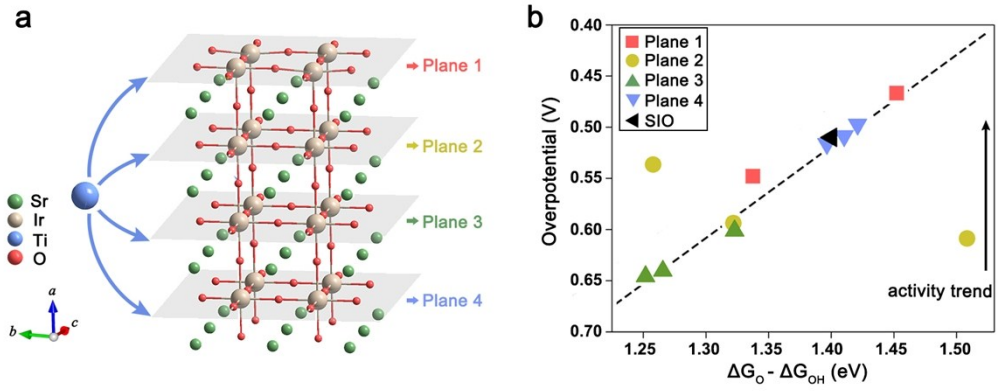

Fig. S9. Schematic of an titanium atom substituting iridium atom on different planes of SIO model. The planes 1-4 represent possible doped planes of SIO model. (b) Negative theoretical overpotential as a function of ΔG_O-ΔG_{HO} for the surface iridium sites in the SIO model with iridium doped in plane 1 (red), plane 2 (yellow), plane 3 (green), plane 4 (blue), respectively. The overpotential (black) for the surface titanium site in SIO is also shown.

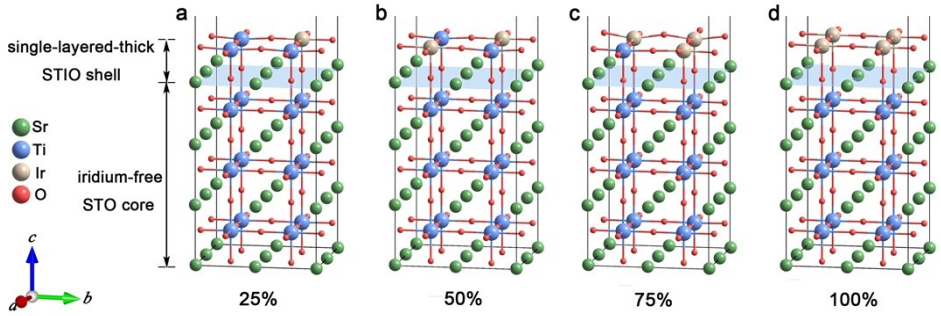

Fig. S10. Structural models of the novel core/shell-type models with different iridium content in the STIO shell. The titanium and iridium sites with different atomic environments are marked on the top views in Fig. 5, inset in main text, and the corresponding free energy for the intermediates are shown in Table S8.

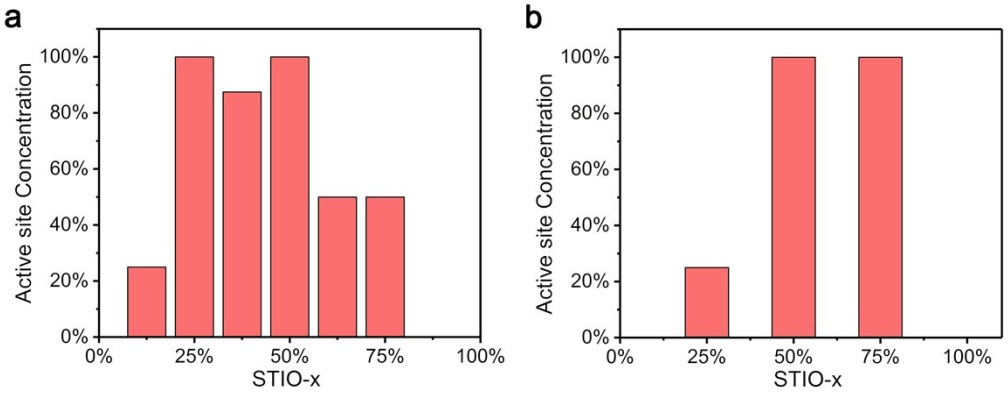

Fig. S11. The active site concentration as a function of the iridium content in (a) STIO models and (b) STIO-shell of the core-shell models. The active site concentration is the ratio of the number of the active sites (the overpotential of the site is similar or lower than that on IrO_2) and the number of all catalytic sites.

Table S1. The possible bulk structures of STIO with iridium content from 25% to 75%, and the related total energies in DFT calculations. The model with the lowest total energy in each iridium content was chosen as the corresponding STIO bulk model.

Iridium content	Sr	Ti	Ir	O
25%	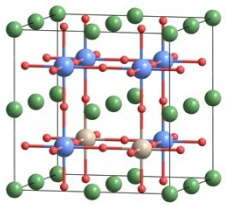 E_{total} = -322.20 eV	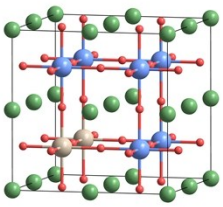 E_{total} = -321.84 eV	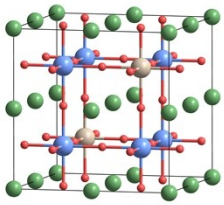 E_{total} = -322.10 eV	
37.5%	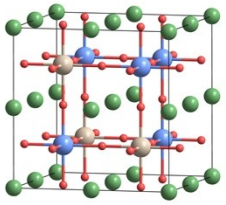 E_{total} = -316.79 eV	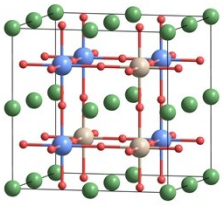 E_{total} = -316.40 eV	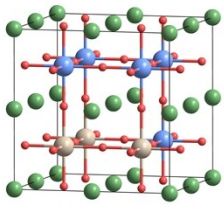 E_{total} = -315.98 eV	
50%	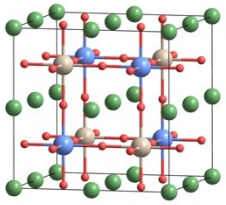 E_{total} = -311.19 eV	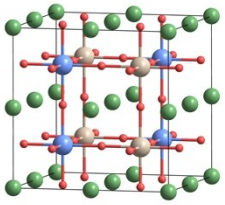 E_{total} = -310.37 eV	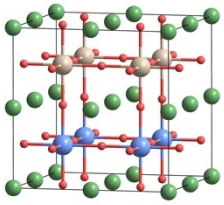 E_{total} = -309.46 eV	
	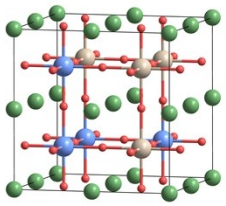 E_{total} = -309.91 eV	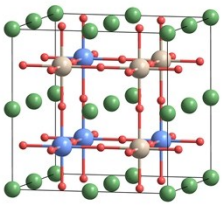 E_{total} = -309.80 eV	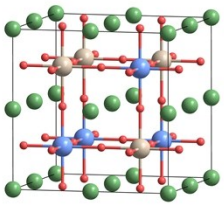 E_{total} = -310.30 eV	
62.5%	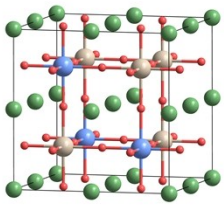 E_{total} = -304.00 eV	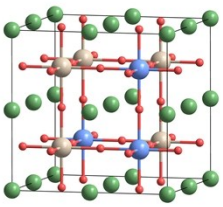 E_{total} = -303.65 eV	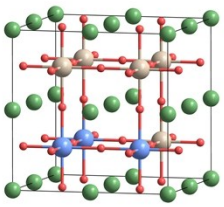 E_{total} = -303.34 eV	
75%	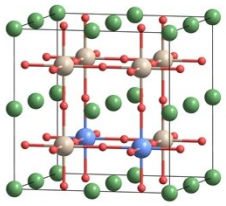 E_{total} = -296.95 eV	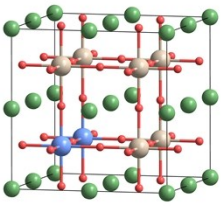 E_{total} = -296.80 eV	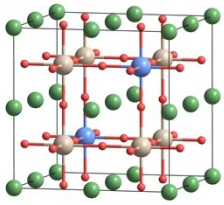 E_{total} = -296.94eV	

Table S2 The optimized lattice parameter of the STIO models with different iridium contents.

Ir %	a	b	c
STO (0%)	7.800	7.800	7.800
12.5%	7.810	7.810	7.810
25%	7.800	7.800	7.856
37.5%	7.828	7.828	7.828
50%	7.840	7.840	7.840
62.5%	7.860	7.860	7.860
75%	7.891	7.891	7.867
87.5%	7.901	7.901	7.901
SIO (100%)	7.920	7.920	7.920

Table S3. The free energy for adsorbed X (X = HO, O, HOO), and e_g–filling on different surface titanium sites (Fig. S2) in the STIO models. The corresponding iridium content in STIO are shown.

	ΔG_{HO*} (eV)	ΔG_{O*} (eV)	ΔG_{HOO*} (eV)	η_{OER} (V)	e_g-filling	note
Ti (STO)	1.37	4.05	4.74	1.45	0.97	*
Ti^{1} (12.5%)	0.94	3.23	4.43	1.06	0.96	
Ti^{2} (12.5%)	1.09	3.04	4.47	0.72	0.92	*
Ti^{3} (25%)	1.23	2.93	4.51	0.47	0.88	*
Ti^{4} (37.5%)	0.86	2.62	4.30	0.53	0.89	*
Ti^{5} (37.5%)	0.94	2.95	4.42	0.78	0.96	
Ti^{6} (37.5%)	1.10	2.93	4.44	0.6	0.88	
Ti^{7} (37.5%)	0.91	2.50	4.29	0.56	0.85	
Ti^{8} (50%)	0.85	2.45	4.25	0.57	0.85	*
Ti^{9} (62.5%)	0.53	2.09	4.06	0.74	0.83	
Ti^{10} (62.5%)	0.85	2.57	4.29	0.49	0.85	*
Ti^{11} (75%)	0.36	2.00	3.84	0.61	0.82	*
Ti^{12} (87.5%)	-0.15	1.24	3.26	0.79	0.78	*

* The most active titanium site in STIO with the corresponding iridium content.

Table S4. The free energy for adsorbed X (X = HO, O, HOO) on different surface iridium sites (Fig. S2) in the STIO models. The corresponding iridium content in STIO are shown.

	ΔG_{HO*} (eV)	ΔG_{O*} (eV)	ΔG_{HOO*} (eV)	η_{OER} (V)	e_g-filling	note
Ir1 (12.5%)	0.22	1.63	3.27	0.42	1.94	*
Ir2 (25%)	0.17	1.57	3.18	0.51	1.91	*
Ir3 (37.5%)	0.16	1.36	3.18	0.59		
Ir4 (37.5%)	0.06	1.50	3.13	0.56	1.91	*
Ir5 (50%)	0.10	1.46	3.14	0.55	1.90	*
Ir6(62.5%)	-0.15	1.44	2.89	0.80		
Ir7 (62.5%)	-0.16	1.05	2.91	0.78		
Ir8 (62.5%)	0.08	1.58	3.19	0.50	2.57	*
Ir9 (62.5%)	0.05	1.45	3.12	0.57		
Ir10 (75%)	-0.21	1.02	2.73	0.96	1.77	*
Ir11 (87.5%)	-0.78	0.57	2.32	1.37		
Ir12 (87.5%)	-0.44	1.02	2.75	0.94	2.51	*
Ir (SIO)	0.44	1.84	3.58	0.51	2.53	*

* The most active iridium site in STIO with the corresponding iridium content.

Table S5. The free energy for adsorbed X (X = HO, O, HOO) on the Ti and Ir sites on 1ML HO* covered surface for STO, STIO-25% and STIO-50%.

	ΔG_{HO*} (eV)	ΔG_{O*} (eV)	ΔG_{HOO*} (eV)	η_{OER} (V)
STO	1.92	4.65	4.87	1.5
Ti$^{\text{ə}}$(25%)	0.76	2.53	4.31	0.55
Ti^{8}(50%)	1.20	3.11	4.51	0.68
Ir$^{\text{ə}}$ (25%)	-0.10	1.29	3.09	0.61
Ir$^{\text{ɔ}}$ (50%)	-0.05	1.22	3.09	0.64

Table S6. The free energy for adsorbed X (X = HO, O, HOO) on different surface titanium and iridium sites (Fig. S7) in the STO models with iridium doped in the possible 4 planes.

	ΔG_{HO*} (eV)	ΔG_{O*} (eV)	ΔG_{HOO*} (eV)	η_{OER} (V)
Ir_a (plane 1)	0.17	1.61	3.24	0.45
Ti_a (plane 1)	0.84	3.16	4.32	1.09
Ti_b (plane 1)	0.98	2.95	4.38	0.74
Ti_c (plane 2)	1.09	3.42	4.59	1.1
Ti_d (plane 2)	1.24	3.73	4.71	1.26
Ti_e (plane 2)	1.15	3.67	4.65	1.29
Ti_f (plane 3)	1.27	3.89	4.69	1.39
Ti_g (plane 3)	1.30	3.94	4.71	1.41
Ti_h (plane 3)	1.30	3.94	4.71	1.41
Ti_i (plane 4)	1.31	3.97	4.72	1.43
Ti_j (plane 4)	1.30	4.00	4.71	1.47
Ti_k (plane 4)	1.31	3.99	4.71	1.45

Table S7. The free energy for adsorbed X (X = HO, O, HOO) on different surface titanium and iridium sites (Fig. S8) in the SIO models with titanium doped in the possible 4 planes.

	ΔG_{HO*} (eV)	ΔG_{O*} (eV)	ΔG_{HOO*} (eV)	η_{OER} (V)
Ti_l (plane 1)	0.76	2.23	4.16	0.70
Ir_b (plane 1)	0.18	1.52	3.29	0.55
Ir_c (plane 1)	0.32	1.77	3.22	0.47
Ir_d (plane 2)	0.40	1.72	3.54	0.59
Ir_e (plane 2)	0.28	1.54	3.30	0.54
Ir_f (plane 2)	-0.01	1.50	3.08	0.61
Ir_g (plane 3)	0.31	1.56	3.44	0.65
Ir_h (plane 3)	0.28	1.60	3.43	0.60
Ir_i (plane 3)	0.43	1.69	3.56	0.64
Ir_j (plane 4)	0.46	1.85	3.60	0.52
Ir_k (plane 4)	0.48	1.89	3.63	0.51
Ir_l (plane 4)	0.46	1.88	3.61	0.50

Table S8. The free energy for adsorbed X (X = HO, O, HOO) and overpotentials different surface titanium and iridium sites (Fig. S10) in the single-layered-thick STIO shell of the novel core/shell-type models.

	ΔG_{HO*} (eV)	ΔG_{O*} (eV)	ΔG_{HOO*} (eV)	η_{OER} (V)
Ir1 (25%)	0.17	1.61	3.24	0.45
Ti1 (25%)	0.84	3.16	4.32	1.09
Ti2 (25%)	0.98	2.95	4.38	0.74
Ir2 (50%)	0.13	1.61	3.19	0.5
Ti3 (50%)	1.14	2.97	4.47	0.6
Ir3 (75%)	-0.03	1.60	3.17	0.52
Ir4 (75%)	-0.09	1.41	3.06	0.63
Ti4 (75%)	0.75	2.62	4.22	0.64
Ir5 (100%)	-0.50	0.68	2.52	1.17

Table S9. The reaction energy (ΔE) and the corresponding zero-point energy (*ZPE*) for oxygen-related intermediates (HO*, O*, and HOO*) adsorbed on each adsorbed sites.

	ΔE_{HO*} (eV)	*ZPE* (HO*)	ΔE_{O*} (eV)	*ZPE* (O*)	ΔE_{HOO*} (eV)	*ZPE* (HOO*)
Ti (STO)	1.02	0.33	4.05	0.06	4.36	0.43
Ti① (12.5%)	0.60	0.34	3.23	0.06	4.05	0.43
Ti② (12.5%)	0.75	0.33	3.03	0.07	4.08	0.44
Ti③ (25%)	0.89	0.33	2.92	0.07	4.12	0.44
Ti④ (37.5%)	0.52	0.33	2.61	0.07	3.92	0.43
Ti⑤ (37.5%)	0.60	0.33	2.95	0.06	4.04	0.43
Ti⑥ (37.5%)	0.76	0.33	2.92	0.07	4.06	0.43
Ti⑦ (37.5%)	0.58	0.32	2.48	0.07	3.90	0.44
Ti⑧ (50%)	0.52	0.32	2.44	0.07	3.87	0.43

Ti^{9} (62.5%)	0.19	0.33	2.08	0.07	3.68	0.44
Ti^{10} (62.5%)	0.51	0.32	2.56	0.07	3.91	0.44
Ti^{11} (75%)	0.03	0.32	1.99	0.07	3.45	0.44
Ti^{12} (87.5%)	-0.48	0.33	1.23	0.07	2.87	0.44
Ir^{1} (12.5%)	-0.13	0.35	1.62	0.07	2.87	0.45
Ir^{2} (25%)	-0.19	0.35	1.56	0.07	2.78	0.45
Ir^{3} (37.5%)	-0.21	0.36	1.35	0.07	2.78	0.45
Ir^{4} (37.5%)	-0.32	0.37	1.50	0.07	2.74	0.45
Ir^{5} (50%)	-0.26	0.35	1.45	0.07	2.74	0.45
Ir^{6}(62.5%)	-0.51	0.35	1.42	0.07	2.49	0.45
Ir^{7} (62.5%)	-0.52	0.35	1.04	0.07	2.51	0.44
Ir^{8} (62.5%)	-0.28	0.35	1.57	0.07	2.80	0.44
Ir^{9} (62.5%)	-0.31	0.35	1.44	0.07	2.72	0.45
Ir^{10} (75%)	-0.56	0.34	1.01	0.07	2.33	0.45
Ir^{11} (87.5%)	-1.15	0.36	0.56	0.07	1.92	0.45
Ir^{12} (87.5%)	-0.79	0.34	1.01	0.07	2.35	0.44
Ir (SIO)	0.08	0.35	1.82	0.07	3.19	0.44
Ir_a (plane 1)	-0.18	0.35	1.60	0.07	2.84	0.45
Ti_a (plane 1)	0.5	0.33	3.15	0.07	3.94	0.43
Ti_b (plane 1)	0.65	0.33	2.94	0.07	4.00	0.43
Ti_c (plane 2)	0.77	0.32	3.42	0.06	4.22	0.42
Ti_d (plane 2)	0.90	0.34	3.74	0.05	4.32	0.43
Ti_e (plane 2)	0.81	0.34	3.68	0.05	4.25	0.45
Ti_f (plane 3)	0.94	0.33	3.88	0.06	4.32	0.42

Ti_g (plane 3)	0.97	0.33	3.93	0.06	4.34	0.42
Ti_h (plane 3)	0.96	0.34	3.93	0.06	4.33	0.42
Ti_i (plane 4)	0.98	0.33	3.97	0.05	4.34	0.43
Ti_j (plane 4)	0.98	0.33	3.98	0.08	4.34	0.42
Ti_k (plane 4)	0.98	0.33	3.98	0.07	4.34	0.42
Ti_l (plane 1)	0.42	0.35	2.16	0.07	3.72	0.44
Ir_b (plane 1)	-0.16	0.34	1.45	0.07	2.85	0.43
Ir_c (plane 1)	-0.02	0.35	1.70	0.06	2.78	0.44
Ir_d (plane 2)	0.06	0.34	1.65	0.07	3.10	0.43
Ir_e (plane 2)	-0.06	0.34	1.47	0.07	2.86	0.44
Ir_f (plane 2)	-0.35	0.34	1.43	0.07	2.64	0.45
Ir_g (plane 3)	-0.03	0.35	1.49	0.07	3.00	0.44
Ir_h (plane 3)	-0.06	0.35	1.53	0.07	2.99	0.45
Ir_i (plane 3)	0.09	0.35	1.62	0.07	3.12	0.45
Ir_j (plane 4)	0.12	0.36	1.78	0.06	3.16	0.44
Ir_k (plane 4)	0.14	0.34	1.82	0.07	3.19	0.44
Ir_l (plane 4)	0.12	0.35	1.81	0.06	3.17	0.43
Ir1 (25%)	-0.18	0.35	1.60	0.07	2.84	0.45
Ti1 (25%)	0.50	0.33	3.15	0.07	3.94	0.43
Ti2 (25%)	0.65	0.33	2.94	0.07	4.00	0.43
Ir2 (50%)	-0.2	0.33	1.6	0.07	2.79	0.45
Ti3 (50%)	0.8	0.34	2.96	0.07	4.08	0.44
Ir3 (75%)	-0.39	0.35	1.6	0.07	2.79	0.44
Ir4 (75%)	-0.45	0.36	1.4	0.07	2.67	0.44

Ti4 (75%)	0.43	0.32	2.62	0.07	3.83	0.44
Ir5 (100%)	-0.88	0.36	0.66	0.07	2.13	0.44

Table S10. The zero-point energy (*ZPE*) and entropy corrections (TS) for the *Gibbs* free energy. For oxygen-related intermediates (HO*, O*, and HOO*), the *ZPE* are shown as the average of the *ZPE* values in Table S9.

	ZPE (eV)	TS(eV)	E (eV)
H_2O	0.59	0.67	-14.24
H_2	0.27	0.41	-6.76
O*	0.07	0	-
HO*	0.34	0	-
HOO*	0.44	0	-

Reference

1 L. Yang, G. Yu, X. Ai, W. Yan, H. Duan, W. Chen, X. Li, T. Wang, C. Zhang, X. Huang, J. S. Chen and X, Zou, *Nat. Commun.* 2018, **9**, 5236.